Anshul Vats, Meenakshi Gupta, Shilpi Pal, Yogita Arora, Neera Aggarwal and Mona Aggarwal*

Channel-aware outage modeling for dual-hop mixed optical wireless communication systems

https://doi.org/10.1515/joc-2025-0142
Received April 17, 2025; accepted May 25, 2025;
published online June 16, 2025

Abstract: This paper presents an in-depth analysis of the outage performance in a dual-hop mixed communication system that combines Free Space Optical (FSO) and Underwater Optical Communication (UWOC) links. The closed-form expressions of the outage probability of the system are derived, while considering practical channel conditions. Specifically, the FSO hop is modeled using Gamma–Gamma statistics to account for pointing errors and atmospheric turbulence, while the UWOC channel follows an Exponential Generalized Gamma (EGG) fading distribution to capture underwater impairments. To validate the analytical results, extensive numerical simulations are conducted, highlighting the impact of key parameters – such as path loss, scintillation, angle-of-arrival variations, water salinity, and pointing instability – on the performance of the considered system.

Keywords: FSO/UOWC system; outage performance; Gamma–Gamma fading; EGG distribution

1 Introduction

Free Space Optical (FSO) communication is a promising point-to-point wireless transmission solution due to its high bandwidth availability in the unregulated spectrum [1]. Compared to traditional Radio Frequency (RF) systems, FSO links offer significantly higher bandwidth and data capacity, making them suitable for applications like cellular backhaul, enterprise/building connectivity, disaster recovery, and redundant backup links [2]. However, the performance of FSO systems is heavily influenced by atmospheric turbulence and pointing errors, and it requires a clear Line-of-Sight (LOS) for optimal operation [3–7].

Mixed RF/FSO systems have been introduced as a strategic solution to combine the distinct advantages of FSO and RF technologies, effectively addressing the limitations of each [8]. While RF links maintain reliability under adverse weather conditions like fog, FSO links provide higher data rates but are more susceptible to atmospheric effects [8–10]. In mixed RF/FSO systems, relay-assisted schemes, especially Amplify-and-Forward (AF) and Decode-and-Forward (DF) protocols, play a crucial role in improving signal transmission from source to destination [11–18]. Recent studies also explore UAV-assisted mixed RF/FSO systems for optimizing outage probability and enhancing secrecy rates [19, 20].

Simultaneously, optical wireless communication is gaining attention in underwater environments due to its wide bandwidth and high data rate capabilities [21]. Underwater Wireless Optical Communication (UWOC) is now an emerging area, especially for applications such as military defense, seismic monitoring, and port security. However, challenges like high signal attenuation and difficult deep-sea conditions make reliable data transfer a complex task. As such, mixed communication systems combining FSO and UWOC links have shown potential in overcoming these limitations, providing robustness across different channel conditions.

Recent works on mixed RF/UWOC systems focus on relay-based architectures for enhanced performance. For example, UAV-assisted RF/UWOC systems have been proposed to optimize metrics like outage probability (OP), average bit error rate (ABER), and secrecy rate [22–27]. However, existing mathematical models for ABER remain complex and less intuitive.

Motivated by these advancements and challenges, we propose a dual-hop Decode-and-Forward (DF) relay-based mixed FSO/UWOC system, aiming to harness the advantages

***Corresponding author: Mona Aggarwal**, Department of Multidisciplinary Engineering, North Cap University, Sector 23 A, Gurgaon, Haryana, India, E-mail: monaaggarwal@ncuindia.com
Anshul Vats, ERNET India, Ministry of Electronics and Information Technology (MeitY), Government of India, New Delhi, India, E-mail: nalurajput2@gmail.com
Meenakshi Gupta, Electronics and Communication Engineering Department, Manav Rachna University, Faridabad, Haryana, India, E-mail: meenakshigupta@mru.edu.in
Shilpi Pal, Department of Electronics and Communication Engineering, School of Engineering and Technology, IFTM University, Moradabad, Uttar Pradesh, India, E-mail: shilpipalmit@gmail.com
Yogita Arora and Neera Aggarwal, Electronics and Communication Engineering Department, Bharati Vidyapeeth's College of Engineering, New Delhi, India, E-mail: yogitamarora@gmail.com (Y. Arora), neera711@gmail.com (N. Aggarwal)

of both optical and RF communication techniques for robust and efficient data transmission.

1.1 Contribution

This work introduces a dual-hop mixed communication framework integrating FSO and UWOC technologies. In the proposed model, the FSO segment – affected by pointing errors – is characterized using the Gamma–Gamma statistics, while the UWOC link is modeled with an Exponential Generalized Gamma (EGG) model to account for complex underwater channel impairments. The system operates via a decode-and-forward (DF) relay that first receives optical signals from a distant source over the FSO link and then transmits the decoded data to the final destination through the UWOC channel. To assess the performance of the system, the cumulative distribution function (CDF) of the overall signal-to-noise ratio (SNR) is derived and utilized to formulate a closed-form expression for the outage probability. The analysis is extended to the high-SNR region, and the theoretical findings are corroborated through detailed numerical simulations. The study also examines the influence of key environmental and system parameters, including atmospheric turbulence, pointing inaccuracies, path loss, angle-of-arrival deviations, salinity levels, multipath effects, and optical scattering caused by air bubbles and temperature gradients in the aquatic medium.

Section 2 outlines the architecture of the proposed dual-hop communication system along with the channel modeling for both FSO and UWOC links. Detailed outage probability analysis is presented in Section 3, followed by the asymptotic analysis under high SNR conditions in Section 4. Numerical results are presented in Section 5 to validate the analytical findings. Finally, the conclusions are summarized in Section 6.

2 System modeling

Figure 1 illustrates the architecture of a dual-hop mixed communication system integrating FSO and UWOC technologies, operating with a DF relaying strategy. In this setup, the source node (S), located at a remote point, initiates the transmission of data signals intended for the destination node (D). Due to the presence of environmental barriers and considerable distance, direct transmission between S and D is not feasible. To overcome this limitation, a DF relay (R) facilitates the communication process.

The relay node R is mounted on a floating platform, such as a diver's boat. During the first hop, the source S sends the data to the relay R through a free-space optical (FSO) link. The relay decodes the received signal, transforms the data into a visible light signal, and forward it through a UWOC link to reach the destination node D, which represents divers operating beneath the ocean surface. It is assumed that the UWOC channel remains static, and any Doppler effects are considered negligible in this model.

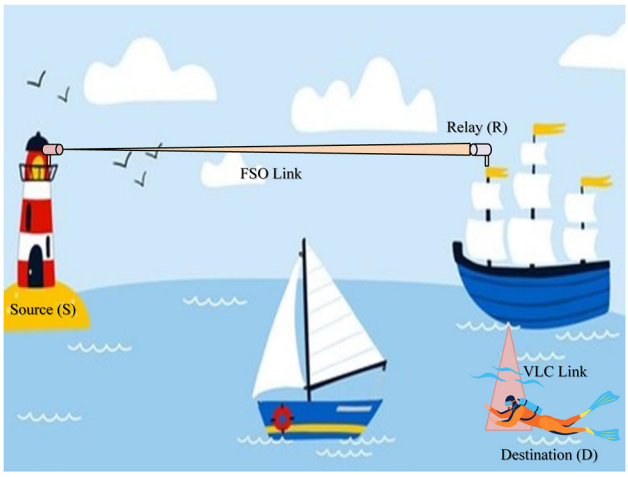

Figure 1: Dual-hop mixed FSO/UWOC system.

In the proposed dual-hop mixed FSO/UWOC communication system, the characteristics of each channel are modeled to reflect real-world environmental effects. The first hop is characterized using the Gamma–Gamma model, which accounts for the influence of pointing errors, atmospheric turbulence, and angle-of-arrival (AOA) variations, denoted by θ_{FOV}. These factors significantly affect signal integrity during aerial transmission.

Further, the underwater segment of the communication system is modeled using the Exponentiated Generalized Gamma (EGG) distribution to capture the statistical behavior of the UWOC channel. In this environment, signal degradation is predominantly influenced by absorption and scattering effects, which have a much greater impact than other disturbances like temperature-induced turbulence or air bubbles. By incorporating this channel model, the system more accurately reflects the actual transmission conditions encountered below the water surface.

2.1 FSO link

The first hop is modeled using the Gamma–Gamma fading distribution, which incorporates the effects of AOA variations in the FSO beam. Recognized for its analytical tractability and ability to accurately represent composite turbulence effects,

the Gamma–Gamma model serves as a widely accepted statistical framework for FSO channels [4]. The probability density function (PDF) of the instantaneous electrical SNR, denoted by $f_{\gamma_{FSO}}(\gamma)$, is expressed as derived in [6, 28].

$$\begin{aligned} f_{\gamma FSO}(\gamma) &= \exp\left(-\frac{\theta_{FOV}^2}{2\sigma_\theta^2}\right) + \left[1-\exp\left(-\frac{\theta_{FOV}^2}{2\sigma_\theta^2}\right)\right] \\ &\times \left[\frac{\zeta^2 \gamma_T^{-1}}{2\Gamma(\alpha_f)\Gamma(\beta_f)}\right. \\ &\left.\times G_{1,3}^{3,0}\left(\frac{\alpha_f\beta_f}{A_o h_l}\left(\sqrt{\frac{\gamma}{\bar{\gamma}_{FSO}}}\right)\middle|\ \frac{1+\zeta^2}{\zeta^2,\alpha,\beta}\right)\right], \end{aligned} \tag{1}$$

where $\bar{\gamma}_{FSO} = \frac{\left(\rho^2 P_{t_1}^2\right)}{\sigma_{n_1}^2}$, P_{t_1} is source transmitted optical power, ρ is optical-to-electrical efficiency, pointing error $\zeta = \frac{w_e}{2\sigma_s}$, σ_θ^2 is the variance of $T_x - R_x$ misalignment orientation. α_f and β_f are the atmospheric turbulence parameters, and $\Gamma(\cdot)$ is the standard Gamma function. $A_0 = erf^2(v)$, where $erf(\cdot)$ is the error function [29]. Integrating (1) using [30, Eq (07.34.21.0084.01)], the analytical expression for the CDF of instantaneous SNR of the FSO link can be written as

$$\begin{aligned} F_{\gamma FSO}(\gamma) &= \exp\left(-\frac{\theta_{FOV}^2}{2\sigma_\theta^2}\right) + \left[1-\exp\left(-\frac{\theta_{FOV}^2}{2\sigma_\theta^2}\right)\right] \\ &\times \left[\frac{\zeta^2}{\Gamma(\alpha_f)\Gamma(\beta_f)}\right. \\ &\left.\times G_{2,4}^{3,1}\left(\frac{\alpha_f\beta_f}{A_o h_l}\left(\sqrt{\frac{\gamma}{\bar{\gamma}_{FSO}}}\right)\middle|\ \frac{1,1+\zeta^2}{\zeta^2,\alpha,\beta,0}\right)\right]. \end{aligned} \tag{2}$$

2.2 UWOC link modeling

This section focuses on modeling the UWOC link. In this context, it is considered that the primary factors affecting optical signal propagation underwater are absorption and scattering, rather than turbulence induced by temperature gradients or air bubbles. The cumulative fading effects resulting from these phenomena are effectively described using the Exponential Generalized Gamma distribution, which accounts for varying levels of water salinity. The CDF of the instantaneous signal-to-noise ratio (SNR), denoted by $F_{\gamma UW}(\gamma)$, is expressed in Equation (21) of [31].

$$\begin{aligned} F_{\gamma UW}(\gamma) &= wG_{1,2}^{1,1}\left(\frac{1}{\lambda}\left(\frac{\gamma}{\mu_r}\right)^{\frac{1}{r}}\right)\middle|\ \frac{1}{1,0}\right) \\ &+\frac{1-w}{\Gamma(a)}G_{1,2}^{1,1}\left(\frac{1}{b^c}\left(\frac{\gamma}{\mu_r}\right)^{\frac{c}{r}}\middle|\ \frac{1}{a,0}\right), \end{aligned} \tag{3}$$

where w, λ, a, b, c are the parameters of the EGG distribution, the intensity modulation and direct detection (IM/DD) scheme is applied with r equals to 2, and μ_r is the average SNR of the UWOC link. The Tables I and II in [31] provide the parameter values corresponding to different salinity levels and temperature gradients, respectively, under varying concentrations of air bubbles.

3 Outage probability analysis

This section discusses the outage performance of the proposed communication system. For this system, the end-to-end instantaneous SNR at the destination node D, denoted by γ_{DF}, is defined as given in [32].

$$\gamma_{DF} = \min[\gamma_{FSO}, \gamma_{UW}], \tag{4}$$

where, γ_{FSO} and γ_{UW} are the instantaneous SNRs of first and second links, respectively. Using (4), the equivalent CDF of the γ_{DF} can be given [33] as

$$F_{\gamma DF}(\gamma) = 1 - (1 - F_{\gamma FSO}(\gamma))(1 - F_{\gamma UW}(\gamma)). \tag{5}$$

Additionally, the probability of outage serves as a crucial metric in assessing the reliability of communication systems. It is defined as the probability that γ_{DF} falls below a specified threshold value, at which point the system's performance is deemed inadequate. Accordingly, the P_{out}^{DF} can be derived from (5) by putting γ by γ_{th} that is $P_{\text{out}}^{DF}(\gamma_{\text{th}}) = F_{\gamma DF}(\gamma_{\text{th}})$. Therefore, substituting $F_{\gamma FSO}(\gamma)$ and $F_{\gamma UW}(\gamma)$ from (2) and (3), respectively, and putting γ_{th} in place of γ, we obtain the analytical expression for the outage probability of the proposed system shown as

$$\begin{aligned} P_{\text{out}}^{DF} &= 1 - \left[\left[1 - wG_{1,2}^{1,1}\left(\frac{1}{\lambda}\left(\frac{\gamma_{\text{th}}}{\mu_r}\right)^{\frac{1}{r}}\middle|\ \frac{1}{1,0}\right)\right.\right. \\ &\left.-\frac{1-w}{\Gamma(a)}G_{1,2}^{1,1}\left(\frac{1}{b^c}\left(\frac{\gamma_{\text{th}}}{\mu_r}\right)^{\frac{c}{r}}\middle|\ \frac{1}{a,0}\right)\right] \\ &\times \left[1-\exp\left(-\frac{\theta_{FOV}^2}{2\sigma_\theta^2}\right) - \left(1-\exp\left(-\frac{\theta_{FOV}^2}{2\sigma_\theta^2}\right)\right)\right. \\ &\left.\left.\times\left(\frac{\zeta^2}{\Gamma(\alpha_f)\Gamma(\beta_f)}G_{2,4}^{3,1}\left(\frac{\alpha_f\beta_f}{A_o h_l}\left(\sqrt{\frac{\gamma_{\text{th}}}{\bar{\gamma}_{FSO}}}\right)\middle|\ \frac{1,1+\zeta^2}{\zeta^2,\alpha,\beta,0}\right)\right)\right]\right]. \end{aligned} \tag{6}$$

4 Asymptotic analysis

Due to the complexity of the expression for the outage probability in the given system, an asymptotic analysis is

done to gain deeper insight into how channel parameters influence the performance of the system. Assuming that both channel links, i.e., FSO and UWOC are independent and identically distributed, with $\bar{\gamma}_{FSO} = \bar{\gamma}_{UW}$, the overall asymptotic outage probability can be approximated by the sum of the individual asymptotic CDFs corresponding to each link's SNR. In the high SNR regime, this leads to a simplified expression that captures the outage behavior of the proposed dual-hop mixed communication system.

$$P_{\text{out}}^{\infty} \cong F_{\gamma DF}^{\infty}(\gamma_{\text{th}}) \cong F_{\gamma FSO}^{\infty}(\gamma_{\text{th}}) + F_{\gamma UW}^{\infty}(\gamma_{\text{th}}), \tag{7}$$

where $F_{\gamma FSO}^{\infty}(\gamma_{\text{th}})$ and $F_{\gamma UW}^{\infty}(\gamma_{\text{th}})$ are CDF's of both links at high SNR regimes, respectively.

The coding gain is defined as $\left(G_C^{xy}\bar{\gamma}\right)^{-G_D^{xy}}$, where $xy \in \{SR, RD\}$, G_C^{xy} is the coding gain and G_D^{xy} is the diversity order of the link [34]. We need to find out $F_{\gamma RF}^{\infty}(\gamma_{\text{th}})$, $F_{\gamma FSO}^{\infty}(\gamma_{\text{th}})$, and $F_{\gamma UW}^{\infty}(\gamma_{\text{th}})$ one by one as shown below:

4.1 First hop

At high SNR values, the CDF of FSO hop given in (2) can be written by identity [35, Eq (6.2.2)] as

$$\begin{aligned} F_{\gamma FSO}^{\infty}(\gamma) &= A\sum_{k=1}^{6}\frac{\Pi_{j=1}^{6}\Gamma(b_j-b_k)\Gamma(b_k)}{\Pi_{j=2}^{3}\Gamma(a_j-b_k)\Gamma(1+b_k)} \\ &\quad\times B^{b_k/2}\left(\frac{\gamma_{\text{th}}}{\bar{\gamma}}\right)^{\frac{b_k}{2}} \\ &= \left(\frac{X^{\frac{-2}{b_k}}}{\gamma_{\text{th}}}\bar{\gamma}\right)^{\frac{-b_k}{2}}, \end{aligned} \tag{8}$$

where $a_j = a_p(j)$, for $j = 1$ to 3,

$b_7 = 0$,

$b_j = b_q(j)$, $j = 1$ *to* 6,

$a_1 = 1$,

$b_k = \min\{\xi^2, \alpha, \beta\}$,

The constant X is equal to $A\sum_{k=1}^{6}\frac{\Pi_{j=1}^{6}\Gamma(b_j-b_k)\Gamma(b_k)}{\Pi_{j=2}^{3}\Gamma(a_j-b_k)\Gamma(1+b_k)}B^{b_k/2}$,

$A = \left[1 - \exp\left(\frac{-\theta_{FoV}^2}{2\sigma_\theta}\right) \times \frac{2\alpha+\beta-2)}{2\pi\Gamma(\alpha)\Gamma(\beta)}\right]$,

$B = \left(\frac{(\alpha\beta)^2}{16}\right)^{\frac{b_k}{2}}$.

4.2 Second hop

The high snr expression of CDF of second hop given in (3) can be written as in [36] as

$$F_{\gamma UW}^{\infty}(\gamma) \simeq \frac{\omega\gamma_{\text{th}}}{\lambda\bar{\gamma}} + \frac{1-\omega}{\Gamma(a+1)}\left(\frac{\gamma_{\text{th}}}{b\bar{\gamma}}\right)^{ac}. \tag{9}$$

Further, putting values of (8) and (9) in (7) and after some rearrangement, the expression for the outage probability can be given as

$$P_{\text{out}}^{\infty} = \left(\frac{X^{\frac{-2}{b_k}}}{\gamma_{\text{th}}}\bar{\gamma}\right)^{\frac{-b_k}{2}} + \left(\frac{\lambda}{\omega\gamma_{\text{th}}}.\bar{\gamma}\right)^{-1} + \left(\frac{b\Gamma(a+1)}{\gamma_{\text{th}}(1-\omega)}.\bar{\gamma}\right)^{-ac}. \tag{10}$$

The diversity gain and coding gain of the system can be directly derived from the asymptotic outage probability expression given in (10). It is evident that the overall system performance is primarily influenced by the weakest link among the two dominant links. Consequently, the system's diversity gain is determined by $\min(\frac{b_k}{2}, ac)$. Based on this diversity gain, G_D, the system's asymptotic outage performance can be categorized into two distinct cases, as detailed below

(1) Case 1: when only 1 hop is dominating out of the two, the coding gain may be written as

$$G_C = \begin{cases} \dfrac{X^{\frac{-2}{b_k}}}{\gamma_{\text{th}}}, & G_D = \dfrac{b_k}{2} \\ \dfrac{\lambda}{\omega\gamma_{\text{th}}} + \dfrac{b\Gamma(a+1)}{(1-\omega)\gamma_{\text{th}}}, & G_D = ac \simeq 1 \end{cases} \tag{11}$$

(2) Case 2: if both the hops are dominating, the coding gain may be written as

$$G_C = \left\{\frac{1}{3}\left(\frac{\lambda}{\omega\gamma_{\text{th}}} + \frac{b\Gamma(a+1)}{(1-\omega)\gamma_{\text{th}}}\right), G_D = \frac{b_k}{2} = ac \simeq 1. \right. \tag{12}$$

5 Results

For the proposed system, numerical results are presented to evaluate outage probability under both low and high SNR scenarios, considering both fresh and saline water environments affected by air bubbles and temperature gradients. The analysis is based on the use of intensity modulation with direct detection technique. The configuration of the FSO link considers various environmental and system-specific parameters. These include an atmospheric loss coefficient of $h_l = 0.9$, a turbulent link span of $d_{FSO} = 1$ km, and a beam radius measuring $w_{d_1} = 2.5$ m. Pointing instability is modeled with a jitter standard deviation of $\sigma_s = 30$ cm, while atmospheric turbulence is characterized using Gamma–Gamma distribution parameters α_f and β_f set to 5.42 and 3.8. At the relay node, the FSO receiver is equipped with a $\sigma_\theta = 7$ mrad field-of-view, and angular deviations due to arrival fluctuations are modeled with a $\sigma_\theta = 7$ mrad standard deviation. For the UWOC

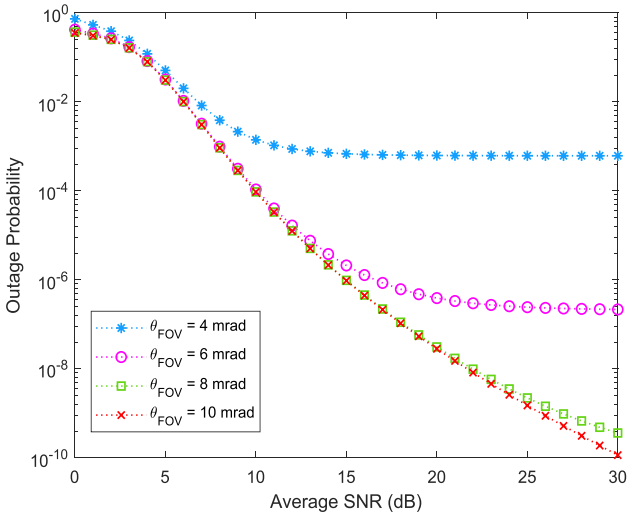

Figure 2: Outage probability variations versus angle of arrival fluctuations.

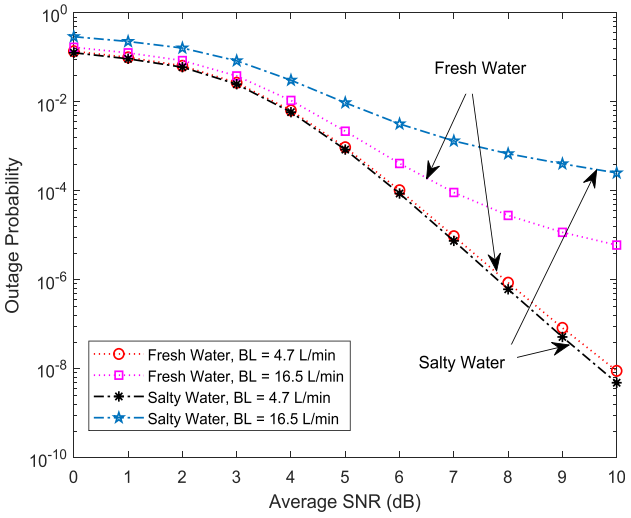

Figure 4: Outage performance of the system in different water types.

segment, parameters such as bubble concentration, thermal gradients, and fading characteristics – denoted by coefficients w, a, b, c and λ are based on the empirical values reported in [31].

Figure 2 depicts the impact of AoA fluctuations on the outage performance of the proposed system. The results reveal that the system experiences degraded performance at lower AoA fluctuation values, indicating a higher sensitivity to misalignment and directional variability in such conditions. However, the outage performance of the system improves significantly with increase in the AOA, θ_{FOV}. For example, at SNR = 25 dB and θ_{FOV} = 4 mrad, the P_{out}^{DF} is equal to 2.499×10^{-3}, and at SNR = 25 dB and θ_{FOV} = 8 mrad, the P_{out}^{DF} is equal to 6.238×10^{-8}. Additionally, it is observed that beyond a certain threshold of average SNR, the influence of AoA fluctuations diminishes, as other channel impairments begin to play a more dominant role in affecting system performance.

Figure 3 illustrates the outage performance of the proposed system under different pointing error conditions, assuming a moderately turbulent FSO channel. The results indicate that as the pointing error parameter ζ increases, the outage probability decreases, signifying enhanced system reliability. This trend highlights that a higher ζ corresponds to reduced pointing error impact, leading to better system performance. Pointing errors typically arise due to

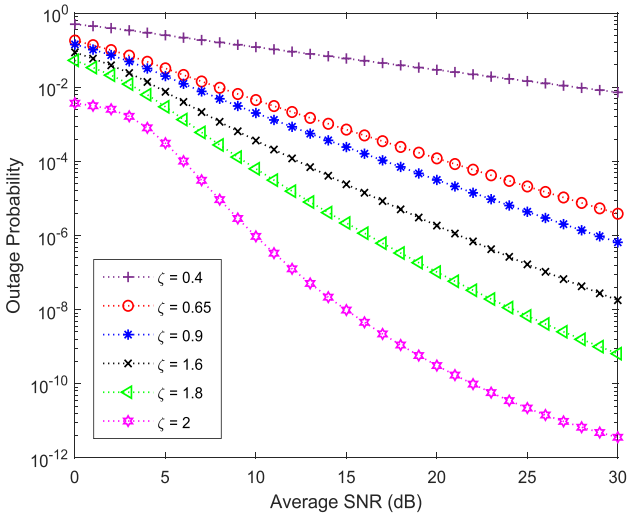

Figure 3: Outage probability of the system with varying pointing errors.

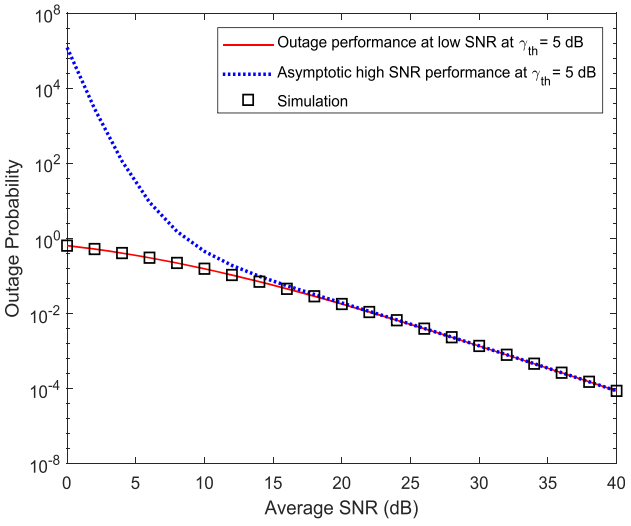

Figure 5: Asymptotic outage probability of the system.

misalignment between the transmitter and receiver or due to atmospheric turbulence-induced beam wander.

Figure 4 illustrates how turbulent underwater conditions affect the outage probability of the mixed FSO/UWOC system for both freshwater and saltwater environments. The results clearly indicate that higher levels of temperature gradients and air bubbles degrade system performance. For instance, in freshwater at an average SNR of 8 dB, increasing the bubble level from 4.7 L/min to 16.5 L/min results in a significant rise in outage probability – from 2.8836×10^{-6} to 3.4207×10^{-4}. A similar trend is observed in saline water, where the outage probability jumps from 2.2815×10^{-6} to 2.0146×10^{-3} under the same bubble level variation. These findings highlight the sensitivity of UWOC links to environmental fluctuations, especially in high-bubble and high-gradient scenarios.

Figure 5 presents the outage probability of the dual-hop FSO/UWOC system across both low and high SNR regimes. The analysis is carried out under moderate atmospheric turbulence, considering saline water conditions with minimal bubble presence and temperature variation. A pointing error of =2 and an angle-of-arrival fluctuation of =7 mrad are assumed. The close alignment between the theoretical results, asymptotic analysis, and Monte Carlo simulations confirms the accuracy and validity of the proposed analytical model for the system's performance evaluation.

6 Conclusions

This paper explored a novel mixed communication architecture that leverages a UAV-assisted relay to bridge a FSO link and an Underwater Optical Communication link, facilitating reliable connectivity between an elevated terrestrial node and an underwater destination. To assess the system's reliability, exact closed-form expressions for outage probability are derived by analyzing the CDF of the end-to-end SNR. Additionally, the system's outage behavior is investigated under high-SNR conditions to provide deeper performance insights. The theoretical findings are corroborated through numerical simulations, which also highlight the impact of critical factors such as atmospheric attenuation, pointing errors, angle-of-arrival variations, and underwater turbulence on the overall performance of the proposed communication framework.

Research ethics: Not applicable.
Informed consent: Not applicable.
Author contributions: All authors have accepted responsibility for the entire content of this manuscript and approved its submission.
Use of Large Language Models, AI and Machine Learning Tools: None declared.
Conflict of interest: All other authors state no conflict of interest.
Research funding: None declared.
Data availability: Not applicable.

References

1. Soleimani-Nasab E, Uysal M. Generalized performance analysis of mixed RF/FSO cooperative systems. IEEE Trans Wireless Commun 2016; 15:714–27.
2. Al-Habash A, Andrews LC, Philips RL. Mathematical model for the irradiance PDF of a laser beam propagating through turbulent media. Opt Eng J 2001;40:1554–62.
3. Khalighi MA, Uysal M. Survey on free space optical communication: a communication theory perspective. IEEE Commun Surv Tutor 2014;16: 2231–58.
4. Aggarwal M, Garg P, Puri P. Analysis of subcarrier intensity modulation-based optical wireless DF relaying over turbulence channels with path loss and pointing error impairments. IET Commun 2014;8:3170–8.
5. Vats A, Aggarwal M, Ahuja S. End-to-end performance analysis of hybrid VLC-RF system using decode and forward relay in E-health medical applications. Opt Int J Electron Opt 2019:297–310. https://doi.org/10.1016/j.ijleo.2019.03.045.
6. Aggarwal M, Garg P, Puri P. Exact MGF-based performance analysis of dual-hop AF-relayed optical wireless communication systems. J Lightwave Technol 2015;33:1913–19.
7. Puri P, Garg P, Aggarwal M, Sharma PK. Multiple user pair scheduling in bi-directional single relay assisted FSO systems. In: 2014 IEEE international conference on communications (ICC). Sydney, Australia; 2014:3401–5 pp.
8. Bag B, Das A, Ansari IS, Prokes A, Bose C, Chandra A. Performance analysis of hybrid FSO systems using FSO/RF-FSO link adaptation. IEEE Photon J 2018;10:1–17.
9. Khanna H, Aggarwal M, Ahuja S. Further results on the performance improvement in mixed RF-FSO systems using hybrid DF/AF (HDAF) relaying. Trans Emerg Telecommun Technol 2018;29:e3284.
10. Lee E, Park J, Han D, Yoon G. Performance analysis of the asymmetric dual-hop relay transmission with mixed RF/FSO links. IEEE Photon Technol Lett 2011;23:1642–4.
11. Shukla NK, Mayet AM, Vats A, Aggarwal M, Raja RK, Verma R, et al. High speed integrated RF–VLC data communication system: performance constraints and capacity considerations. Phys Commun 2022;50:1–14.
12. Zedini E, Ansari I, Alouini M-S. Performance analysis of mixed Nakagami-m and gamma–gamma dual-hop FSO transmission systems. IEEE Photon J 2015;7:1–20.
13. Anees S, Bhatnagar MR. Performance of an amplify-and-forward dual-hop asymmetric RF–FSO communication system. J Opt Commun Netw 2015;7:124–35.
14. Ansari IS, Yilmaz F, Alouini M. Impact of pointing errors on the performance of mixed RF/FSO dual-hop transmission systems. IEEE Wirel Commun Lett 2013;2:351–4.
15. Zedini E, Ansari IS, Alouini M. Unified performance analysis of mixed line of sight RF-FSO fixed gain dual-hop transmission systems. In: proceedings of IEEE wireless communications and networking conference (WCNC). New Orleans, LA, USA; 2015:46–51 pp.

16. Miridakis NI, Matthaiou M, Karagiannidis GK. Multiuser relaying over mixed RF/FSO links. IEEE Trans Commun 2014;62:1634–45.
17. Anees S, Bhatnagar MR. Performance evaluation of decode-and-forward dual-hop asymmetric radio frequency free space optical communication system. IET Optoelectron 2015;9:232–40.
18. Miridakis NI, Matthaiou M, Karagiannidis GK. Multiuser dual-hop relaying over mixed RF/FSO links. In: Proceedings of IEEE international conference on communications (ICC). Sydney, NSW, Australia; 2014: 3389–94 pp.
19. Yang L, Yuan J, Liu X, Hasna MO. On the performance of LAP-based multiple-hop RF/FSO systems. IEEE Trans Aero Electron Syst 2019;55: 499–505.
20. Tatar Mamaghani M, Hong Y. On the performance of low-altitude UAV-enabled secure AF relaying with cooperative jamming and SWIPT. IEEE Access 2019;7:153060–73.
21. Hanson F, Radic S. High bandwidth underwater optical communication. Appl Opt 2008;47:277–83.
22. Li S, Yang L, Costa D. Performance analysis of UAV-based mixed RF/UWOC transmission systems. ArXiv, abs/2011.09062 2020.
23. Anees S, Deka R. On the performance of DF based dual-hop mixed RF/UWOC system. In: Proceedings of IEEE 89th vehicular technology conference (VTC2019-spring). Malaysia: Kuala Lumpur; 2019:1–5 pp.
24. Yadav S, Vats A, Aggarwal M, Ahuja S. Performance analysis and altitude optimization of UAV-enabled dual-hop mixed RF-UWOC system. IEEE Trans Veh Technol 2021;70:12651–61.
25. Anees S, Bhatnagar MR. Performance of an amplify-and-forward dual-hop asymmetric RF-FSO communication system. IEEE/OSA J Opt Commun Netw 2015;7:124–35.
26. Lei H, Zhang Y, Park K, Ansari IS, Pan G, Alouini M. On the performance of dual-hop RF-UWOC system. In: Proceedings of IEEE international conference on communications workshops (ICC workshops). Dublin, Ireland; 2020:1–6 pp.
27. Illi E, Bouanani FE, da Costa DB, Sofotasios PC, Ayoub F, Mezher K, et al. Physical layer security of a dual-hop regenerative mixed RF/UOW system. IEEE Trans Sustain Comput 2021;6:90–104.
28. Vaiopoulos N, Vavoulas A, Sandalidis HG. An assessment of a unmanned aerial vehicle-based broadcast scenario assuming random terrestrial user locations. IET Optoelectron 2021;15:121–30.
29. Safi H, Dargahi A, Cheng J, Safari M. Analytical channel model and link design optimization for ground-to-HAP free-space optical communications. J Lightwave Technol 2020;38:5036–47.
30. Oleg Marichev and Michael Trottd. The mathematical functions site. http://functions.wolfram.com [Accessed 5 Jun 2022].
31. Zedini E, Oubei HM, Kammoun A, Hamdi M, Ooi BS, Alouini M. Unified statistical channel model for turbulence-induced fading in underwater wireless optical communication systems. IEEE Trans Commun 2019;67: 2893–907.
32. Laneman JN, Tse DNC, Wornell GW. Cooperative diversity in wireless networks: efficient protocols and outage behavior. IEEE Trans Inf Theor 2004;50:3062–80.
33. Ikki SS, Aissa S. A study of optimization problem for amplify-and-forward relaying over Weibull fading channels with multiple antennas. IEEE Commun Lett 2011;15:1148–51.
34. Vats A, Aggarwal M, Ahuja S. Outage and error analysis of three hop hybrid VLC/FSO/VLC–based relayed optical wireless communication system. Trans Emerging Telecommun Technil 2019;30:e3544.
35. Dale M. The algebra of random variables. New York: Wiley; 1979, vol 1.
36. Amer M, Al-Eryani Y. Underwater optical communication system relayed by $\alpha - \mu$ fading channel: outage, capacity and asymptotic analysis. arXiv preprint arXiv:1911.04243 2019.